Properties of two-fluid ST equilibria observed in HIST double-pulsing CHI experiments

T. Kanki[1] and M. Nagata[2]

[1]Japan Coast Guard Academy, [2]University of Hyogo

NEXT Workshop

29 - 30 August, 2013; ROHM Plaza, Katsura Campus, Kyoto University, Japan

---

Outline:

-- Helicity-driven spherical system

-- Multi-pulsed coaxial helicity injection (M-CHI)

-- Plasma flow in the double pulsing CHI experiment on HIST

-- Numerical results of two-fluid flowing equilibria

-- Summary

Helicity-driven spherical system

Many experiments on the CHI using a magnetized coaxial plasma gun (MCPG) have been carried out for ST to understand the mechanism of current drive.

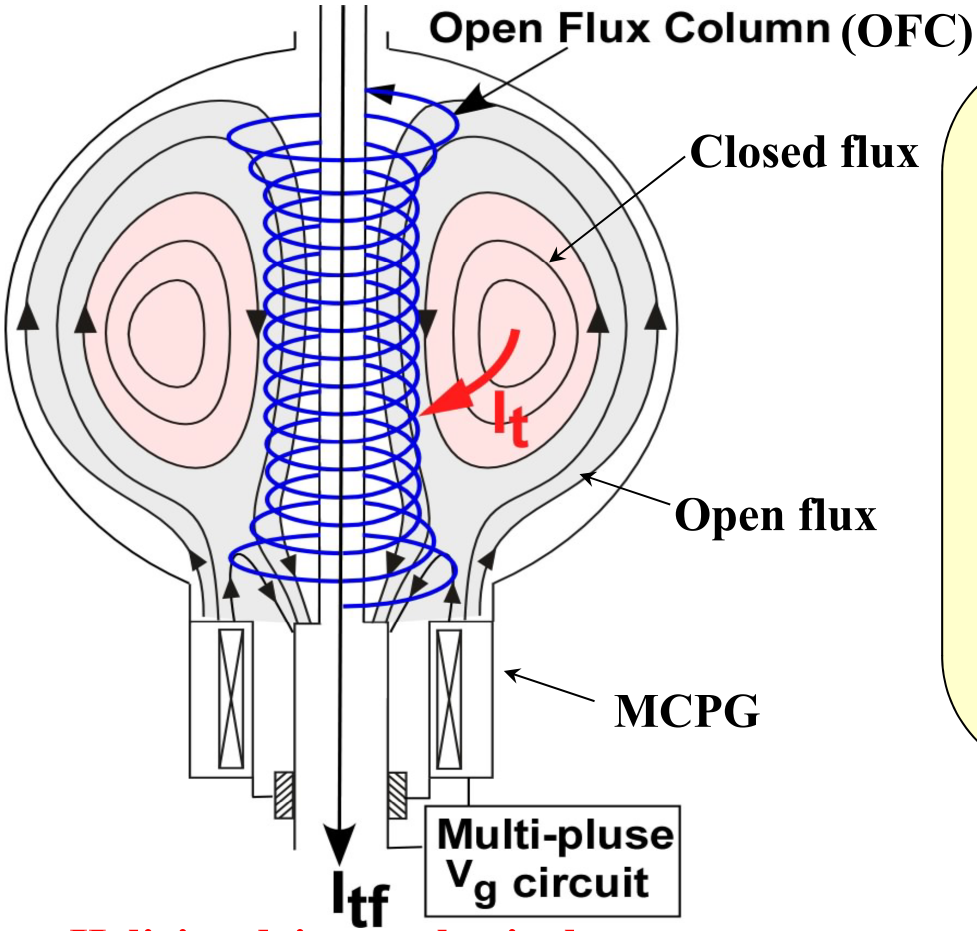

Helicity-driven spherical system

-- Sustainment of the ST configuration by CHI are considered to be due to a ***dynamo*** driven by magnetic fluctuations crossing flux surfaces.

-- In the driven phase which performs the dynamo current drive, the fluctuations deteriorate ***confinement***.

-- In the decay phase after the driven phase, the fluctuations become small, ***allowing closed flux surfaces to form, resulting in good confinement.***

Background and motivation

1. Driven phase: Current drive is performed with allowing the deterioration of confinement.
2. Decay phase: Closed flux surfaces are formed, resulting in good confinement.

↓

The multi-pulsing CHI (M-CHI) scenario aims to achieve simultaneously a quasi-steady sustainment and good confinement by repeating the driven and decay phases [1, 2].

-- The double-pulsing CHI experiment for ST is performed to demonstrate its usefulness in HIST.

-- The poloidal shear flow and the Hall dynamo are observed near the separatrix layer with the steep density gradient in the high field side, due to the ion diamagnetic drift.

→ The two-fluid effects are important!

-- A main purpose of this study is to explore the features of the 2-fluid equilibria observed in HIST on the basis of double-pulsing discharge data such as magnetic field, ion flow velocity, etc.

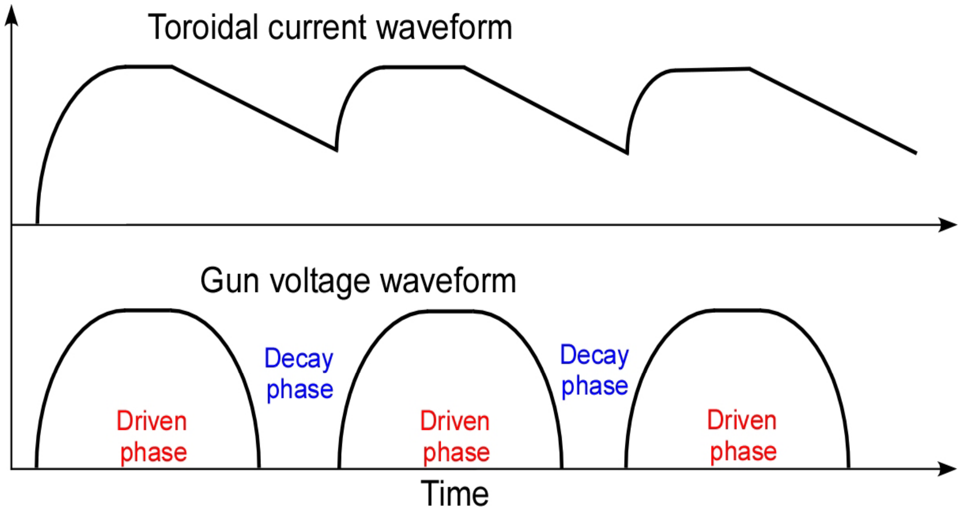

[1] S. Woodruff, et al., PRL **90**, 205002-1 (2004).
[2] E.B. Hooper, PPCF **53**, 085008 (2011).

HIST device and double-pulsing CHI

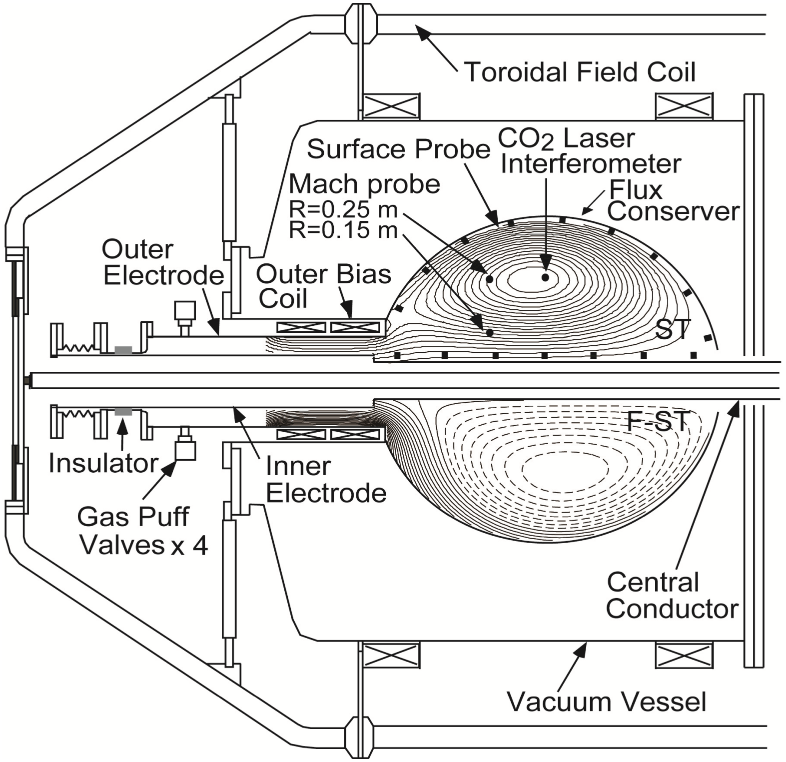

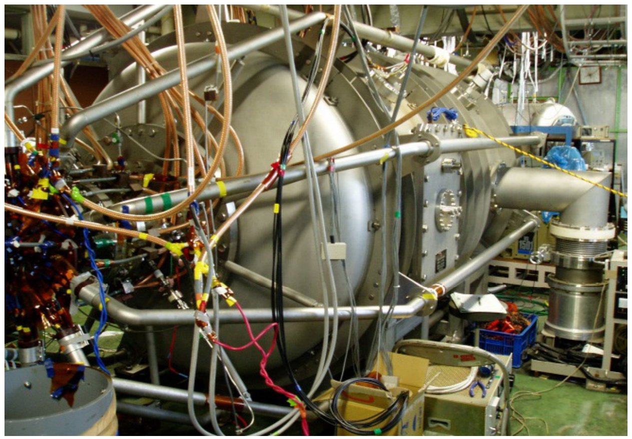

- **HIST parameters**

  $R = 0.3$ m, $a = 0.24$ m, $A = 1.25$
  $n_e = 0.5\text{-}1 \times 10^{20}$ m^{-3}
  $T_{e,}\ T_i = 10\text{-}40$ eV
  $I_t < 150$ kA,
  $S^* = R / l_i \sim 10 \quad l_i = (c / \omega_{pi}) = 2\sim3$ cm

- **TF coil current**

  Spheromak, Low-q ST: $q \sim I_{tf}$ (= 0-30 kA) / $I_t < 1$

  High-q ST: $q \sim I_{tf}$(= ~ 150 kA) / $I_t > 1$

- **Power supply system for double-pulse**

  Formation capacitor banks: V = 3-10 kV, C = 0.6 mF
  Injection current: $I_g \sim 30$ - 60 kA

- **Sustainment capacitor banks**

  First pulse: $V < 900$ V, $C = 336$ mF
  Second pulse: $V < 900$ V, $C = 195$ mF

2nd pulse voltage: $V_g \sim 400$ V
2nd pulse current: $I_g \sim 10\text{-}20$ kA

Double pulsing CHI discharge (High-q)

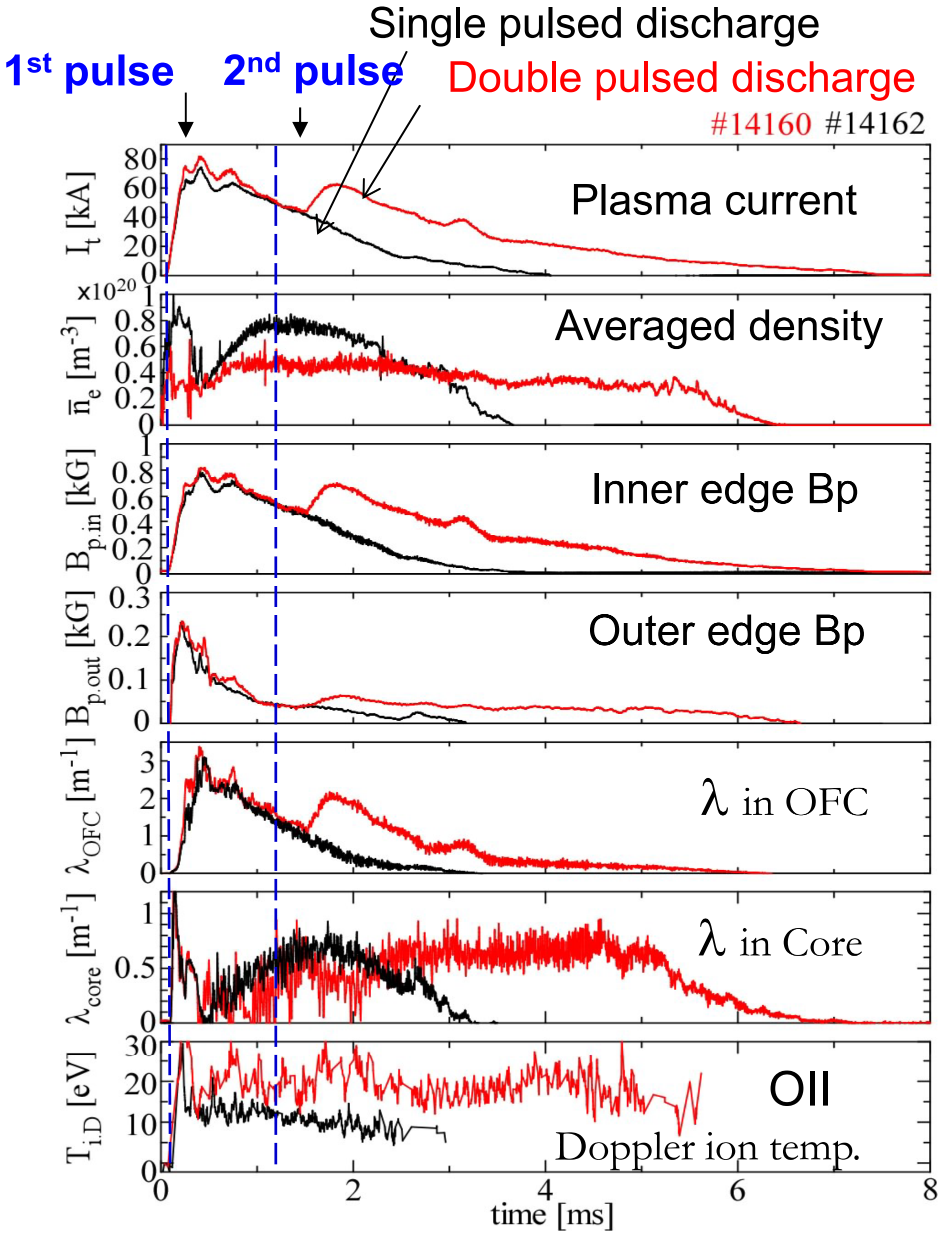

- By secondly pulsing the MCPG at t = 1.5 or 2.5 ms during the partially decay phase, total plasma current is effectively amplified against the resistive decay. The core current density is generated due to dynamo.
- The sustainment time has increased up to 6 -8 ms which is longer than that in the single CHI case.
- The edge λ in the OFC is larger than the core λ, causing helicity transport.

$$\lambda = \mu_0 I_t / \Psi_t$$

- Ion Doppler temperature increases from 20 eV up to 30 eV.

Internal magnetic field profiles

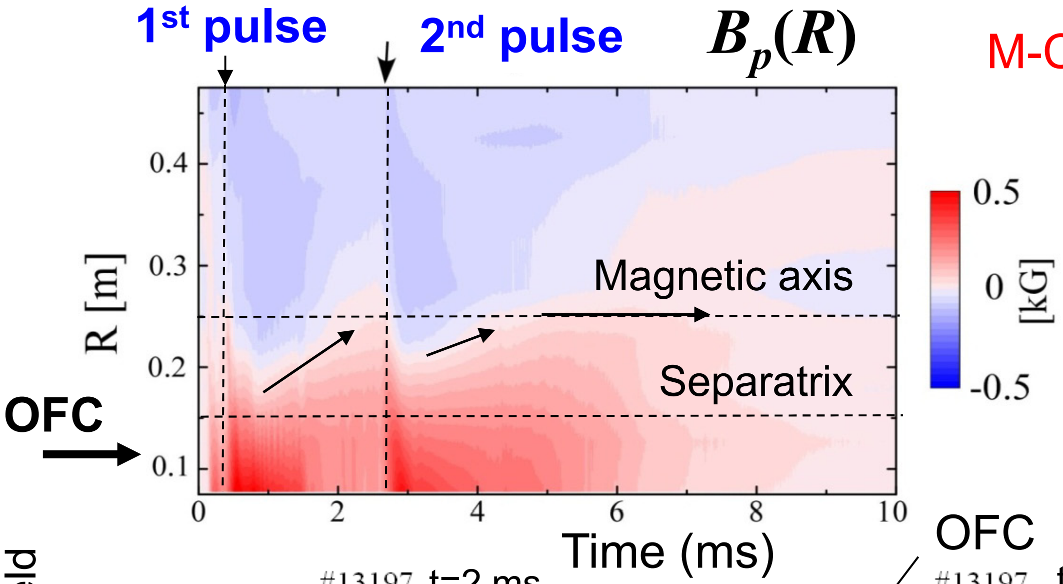

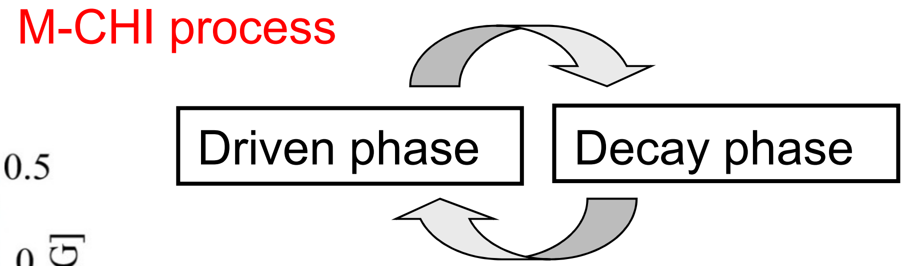

B_p is enhanced in the OFC.
Magnetic axis moves outwardly.
J_t becomes from a hollow to a peaked profile.

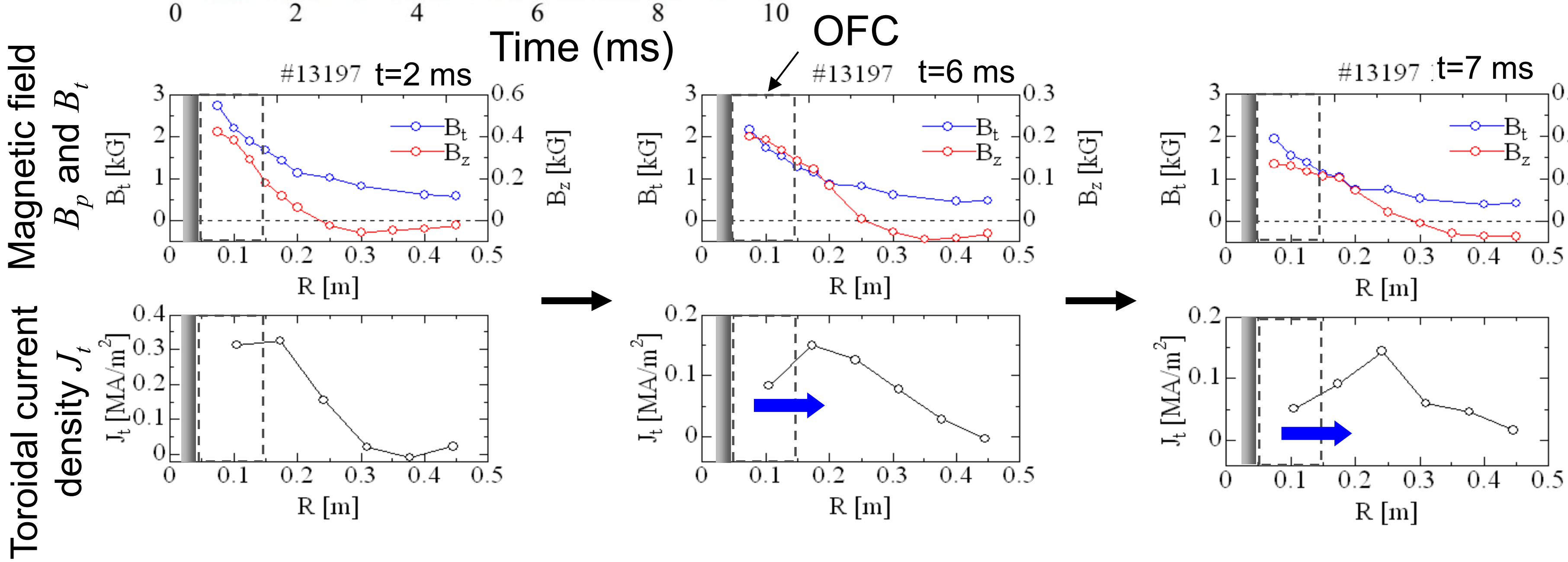

Flow velocity and density profiles

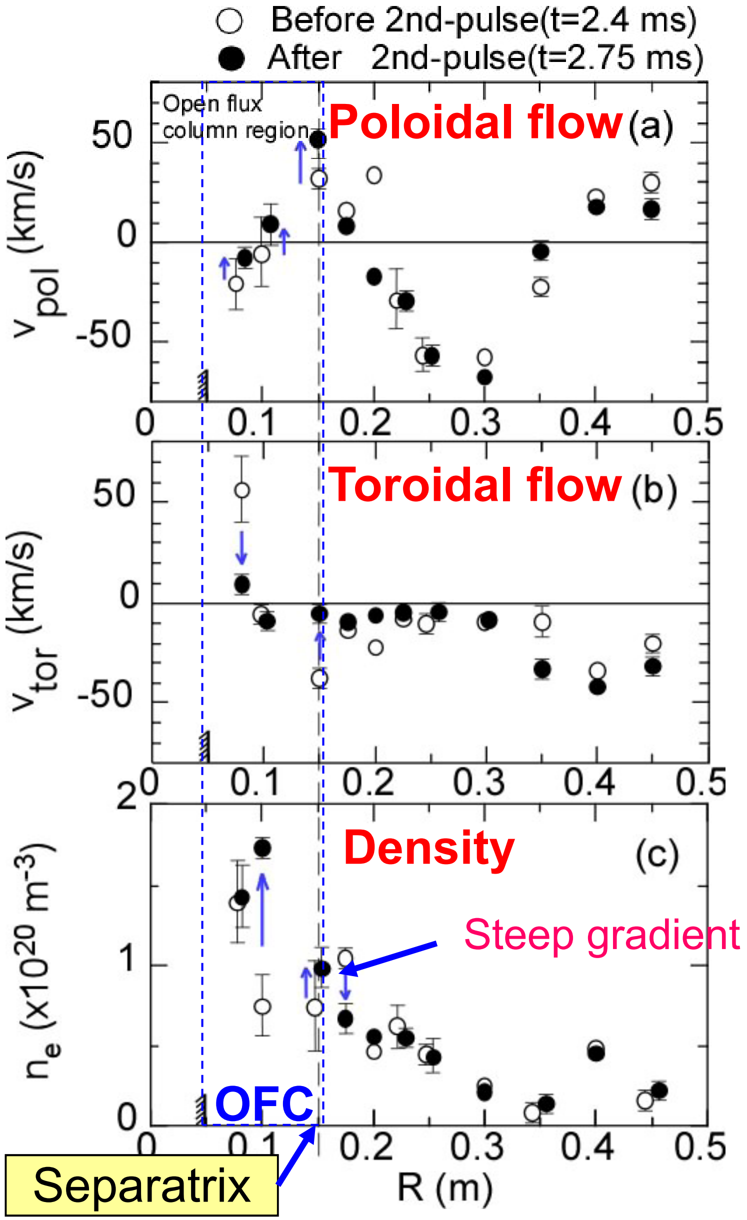

$$v_p = \boxed{\frac{E_r \times B_t}{B^2}} - \boxed{\frac{\nabla p_i \times B_t}{enB^2}}$$

ExB drift Diamagnetic drift

⇩

Poloidal shear flow

Diamagnetic current

⇨ Diamagnetic properties of OFC

⇩

Toroidal field in OFC is observed to be decreased from vacuum field.

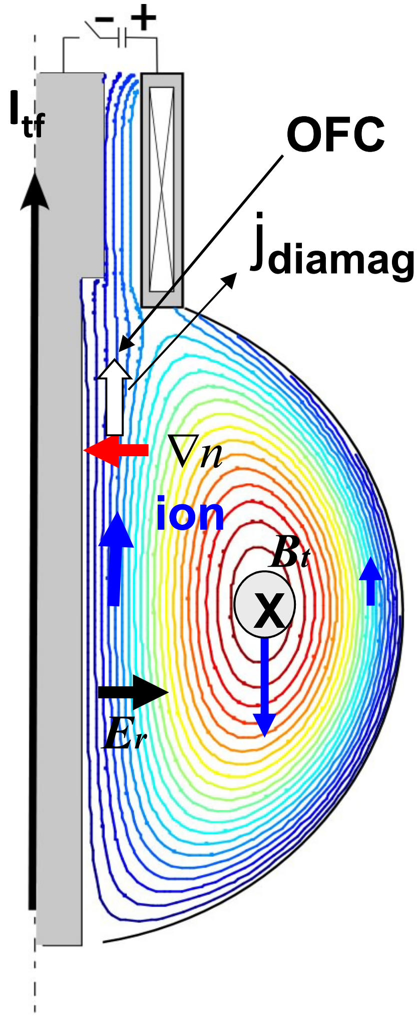

Normalization

We normalize the physical quantities on the basis of the following quantities in HIST.

L: Radius of the flux conserver
0.5 [m]

B_R: Poloidal field at the outer boundary at a midplane 0.05 [T]

n_R: Number density 5×10^{19} [m^{-3}]

Reference values

Alfven velocity: $u_R = B_R / (\mu_0 m_i n_R)^{1/2} = 154$ [km/s]

Temperature: $T_R = B_R^2 / \mu_0 n_R k = 248$ [eV]

Normalized equilibrium equations

Equation of ion motion $\mathbf{u}_i \cdot \nabla \mathbf{u}_i = -\nabla p_i / n + \mathbf{E} + (1/\varepsilon)\mathbf{u}_i \times \mathbf{B}$

Equation of electron motion $0 = -\nabla p_e / n - \mathbf{E} - (1/\varepsilon)\mathbf{u}_e \times \mathbf{B}$

Equation of continuity $\nabla \cdot (n\mathbf{u}_i) = 0 \qquad \nabla \cdot (n\mathbf{u}_e) = 0$

Entropy conservation $\mathbf{u}_i \cdot \nabla s_i = 0 \qquad \mathbf{u}_e \cdot \nabla s_e = 0$

Equations of state $p_i = n^\gamma \exp\left[(\gamma - 1)s_i\right] \qquad p_e = n^\gamma \exp\left[(\gamma - 1)s_e\right]$

Gauss' law for magnetic field $\nabla \cdot \mathbf{B} = 0$

Ampere's law $n(\mathbf{u}_i - \mathbf{u}_e) = \varepsilon \nabla \times \mathbf{B}$

Faraday's law $\nabla \times \mathbf{E} = 0 \quad \Rightarrow \quad \mathbf{E} = -\nabla \phi_E$

Two-fluid parameter: $\varepsilon \equiv \ell_i / L$ $\qquad \ell_i \equiv c / \omega_{pi}$ = ion skin depth

L = system length scale

$\ell_i \propto m_i^{1/2}$, thus ε = an ion inertia effect

HIST	$\varepsilon = 0.0644$
TCS-translation	$\varepsilon = 0.22$
TS-3	$\varepsilon = 0.20$
NSTX	$\varepsilon = 0.034$

Surface variables and functions

Surface variables

electron (and magnetic) surface variable: $\psi(r,z)$ ← poloidal flux function

ion surface variable: $$\mathrm{Y}(r,z) \equiv \psi + \varepsilon r u_\theta$$

toroidal ion flow velocity

Arbitrary surface functions

electron poloidal flow function: $\overline{\psi}_e(\psi)$ ion poloidal flow function: $\overline{\psi}_i(\mathrm{Y})$

$$\Lambda_e(\psi) \equiv \overline{\psi}_e'(\psi) \qquad \Lambda_i(\mathrm{Y}) \equiv \overline{\psi}_i'(\mathrm{Y})$$

electron total enthalpy function: $H_e(\psi)$ ion total enthalpy function: $H_i(\mathrm{Y})$

electron entropy function: $S_e(\psi)$ ion entropy function: $S_i(\mathrm{Y})$

Axisymmetric equilibrium equations

Generalized Grad-Shafranov equations

ion:

$$\underbrace{\overline{\psi}_i' r^2 \nabla \cdot \left(\frac{\overline{\psi}_i'}{n} \frac{\nabla \mathrm{Y}}{r^2} \right)}_{\textit{poloidal flow inertia}} = \underbrace{\frac{r}{\varepsilon} \left(B_\theta \overline{\psi}_i' - n u_\theta \right)}_{\mathbf{u} \times \mathbf{B} \text{ force}} + \underbrace{n r^2 \left(H_i' - T_i S_i' \right)}_{\textit{pressure, flow energy, electric field}}$$

electron:

$$r^2 \nabla \cdot \left(\frac{\nabla \psi}{r^2} \right) = \frac{r}{\varepsilon} \left(B_\theta \overline{\psi}_e' - n u_\theta \right) - n r^2 \left(H_e' - T_e S_e' \right)$$

Problem:

$1/\varepsilon$ singularities

Generalized Bernoulli equations

ion:

$$\underbrace{\frac{\gamma}{\gamma - 1} n^{\gamma - 1} \exp\left[(\gamma - 1) S_i \right]}_{\textit{enthalpy}} + \frac{u^2}{2} + \phi_E = H_i$$

electron:

$$\frac{\gamma}{\gamma - 1} n^{\gamma - 1} \exp\left[(\gamma - 1) S_e \right] - \phi_E = H_e$$

Flexible arbitrary functions for H_α and S_α

$$H_e(\psi) = H_{e0} + (H_{e1} - H_{e0}) \left.\frac{df}{dx}\right|_{\psi - \Delta\psi;\delta_{e1},\delta_{e2}} \qquad H_i(\Upsilon) = H_{i0} + (H_{i1} - H_{i0}) \left.\frac{df}{dx}\right|_{\Upsilon - \Delta\Upsilon;\delta_{i1},\delta_{i2}}$$

$$f(x;\delta_1,\delta_2) = \frac{1}{\delta_1 + \delta_2} \left\{ \begin{array}{cc} \delta_1^2 e^{x/\delta_1}; & x < 0 \\ \delta_1 x + \delta_2 \sqrt{\delta_2^2 + x^2} - \delta_2^2 + \delta_1^2; & x \geq 0 \end{array} \right\}$$

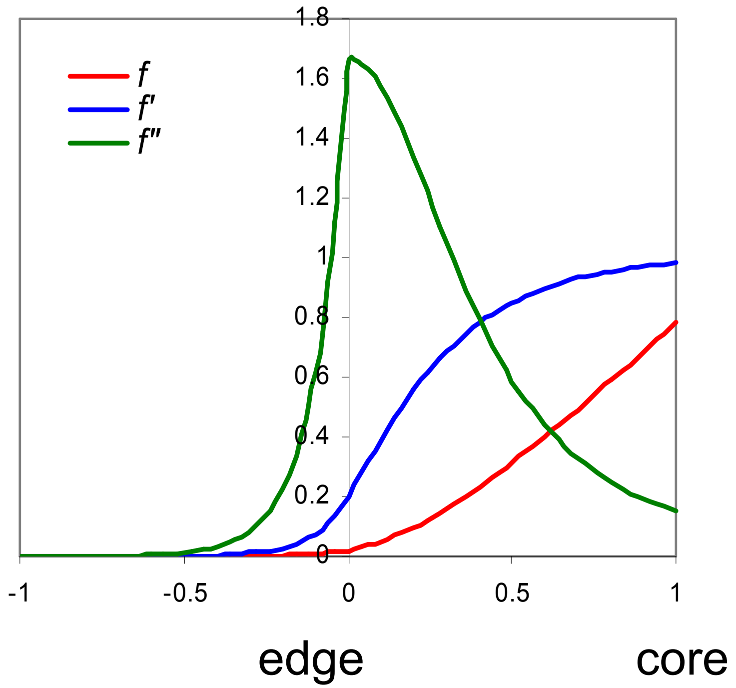

Flexible arbitrary functions for Λ_α

$$\Lambda_e(\psi) = \Lambda_{e0} + (\Lambda_{e1} - \Lambda_{e0}) \left.\frac{df}{dx}\right|_{\psi-\Delta\psi;\delta_{e0},\delta_{e1},\delta_{e2}} \qquad \Lambda_i(\Upsilon) = \Lambda_{i0} + (\Lambda_{i1} - \Lambda_{i0}) \left.\frac{df}{dx}\right|_{\Upsilon-\Delta\Upsilon;\delta_{i0},\delta_{i1},\delta_{i2}}$$

$$f(x;\delta_0,\delta_1,\delta_2) = \begin{cases} -\dfrac{1}{\delta_0\delta_1}\left[\dfrac{\delta_0^4}{12}\left(1-\dfrac{2\delta_1}{\delta_0}\right) + x^2\left\{\dfrac{\delta_0\delta_1}{2} + x\left(\dfrac{\delta_0+\delta_1}{3} + \dfrac{x}{4}\right)\right\}\right]; & x < 0 \\ -\dfrac{\delta_0^3}{12\delta_1}\left(1-\dfrac{2\delta_1}{\delta_0}\right) - \delta_2\left\{x - \delta_2 \log\left(1+\dfrac{x}{\delta_2}\right)\right\}; & x \geq 0 \end{cases}$$

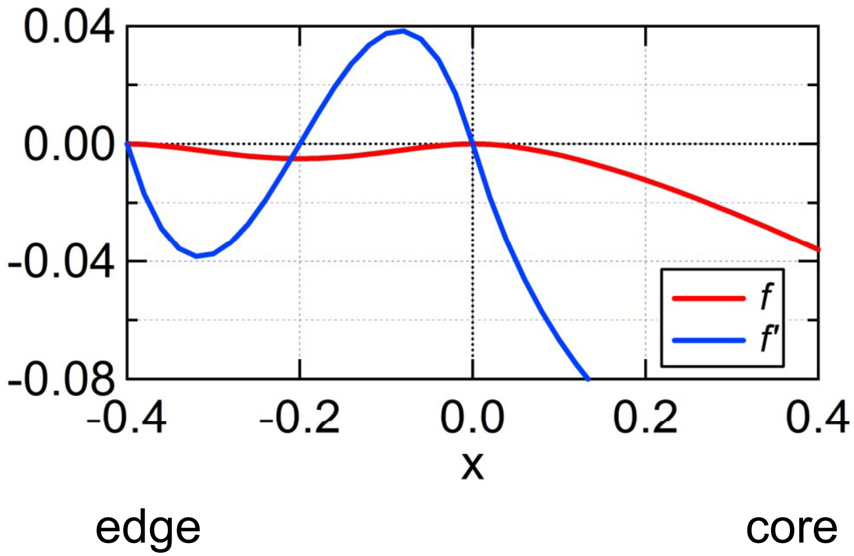

Neaby-fluids ordering

-- Two-fluid parameter as $\varepsilon << 1$

-- Adopt two postulates:

a) Toroidal magnetic field $B_\theta \leq O(1)$ formally

b) Toroidal flow velocity $u_\theta \leq O(1)$ formally

-- Require two arbitrary surface functions:

$\Lambda_e(\ldots)$ and $\Lambda_i(\ldots)$ must differ only to $O(\varepsilon)$

$$\Lambda_e(\psi) \equiv \overline{\psi}_e'(\psi) = F(\psi) \qquad \Lambda_i(\mathrm{Y}) \equiv \overline{\psi}_i'(\mathrm{Y}) = F(\mathrm{Y}) + \varepsilon G'(\mathrm{Y})$$

$$G'(\mathrm{Y}) = [\Lambda_i(\mathrm{Y}) - \Lambda_e(\mathrm{Y})]/\varepsilon \qquad G(\mathrm{Y}) = G_0 + \frac{1}{\varepsilon}\left[\int \Lambda_i(\mathrm{Y})\mathrm{dY} - \int \Lambda_e(\psi)\mathrm{d}\psi\right]$$

-- $GG' < 0$ → diamagnetism, $GG' > 0$ → paramagnetism

L.C. Steinhauer and A. Ishida, Phys. Plasmas **13**, 052513 (2006)

Numerical model

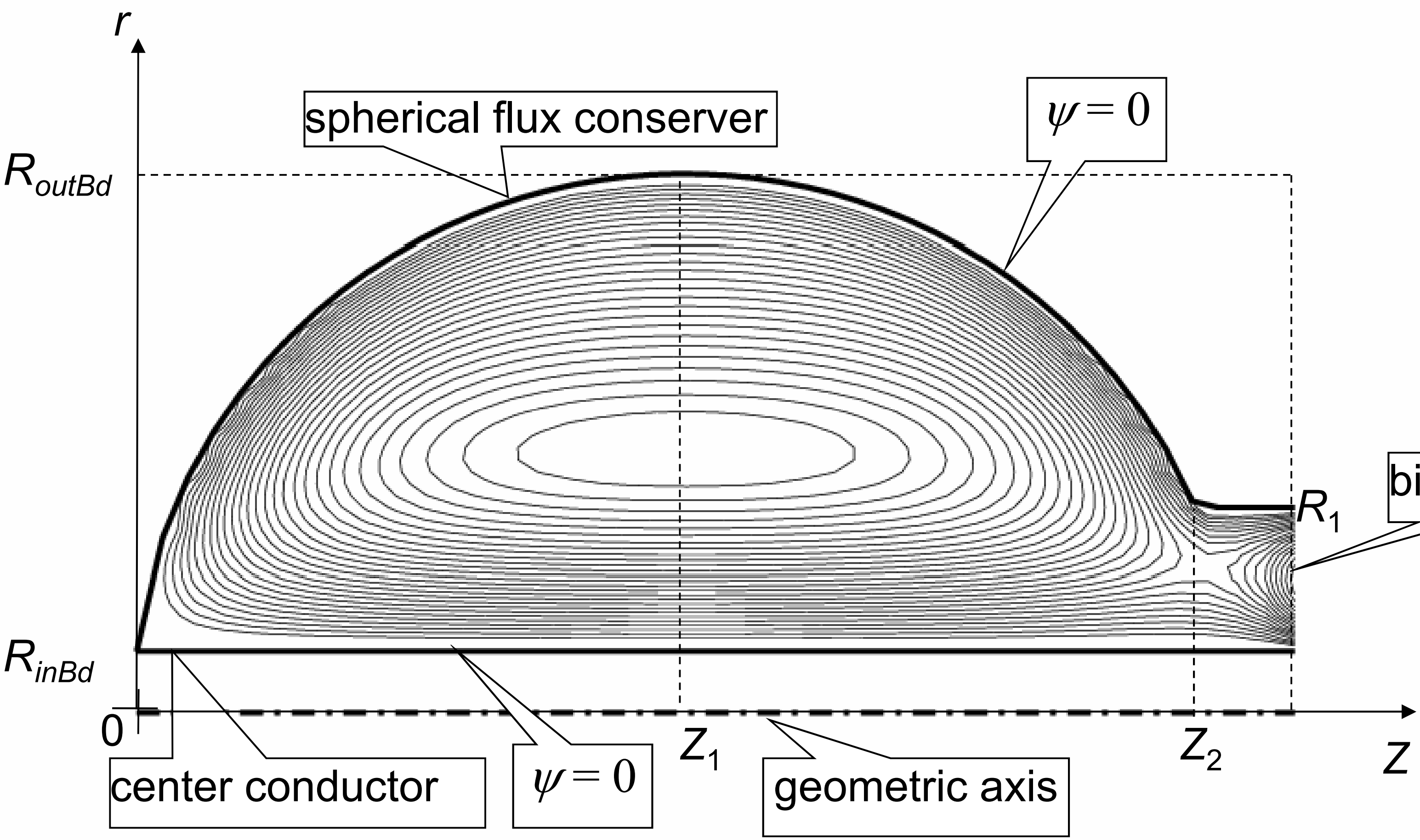

Function form of bias flux: $$\psi_{\text{bias}}(r) = \frac{4\psi_s}{(R_1 - R_{inBd})^2}(r - R_{inBd})(R_1 - r)$$

Poloidal flux contours and safety factor

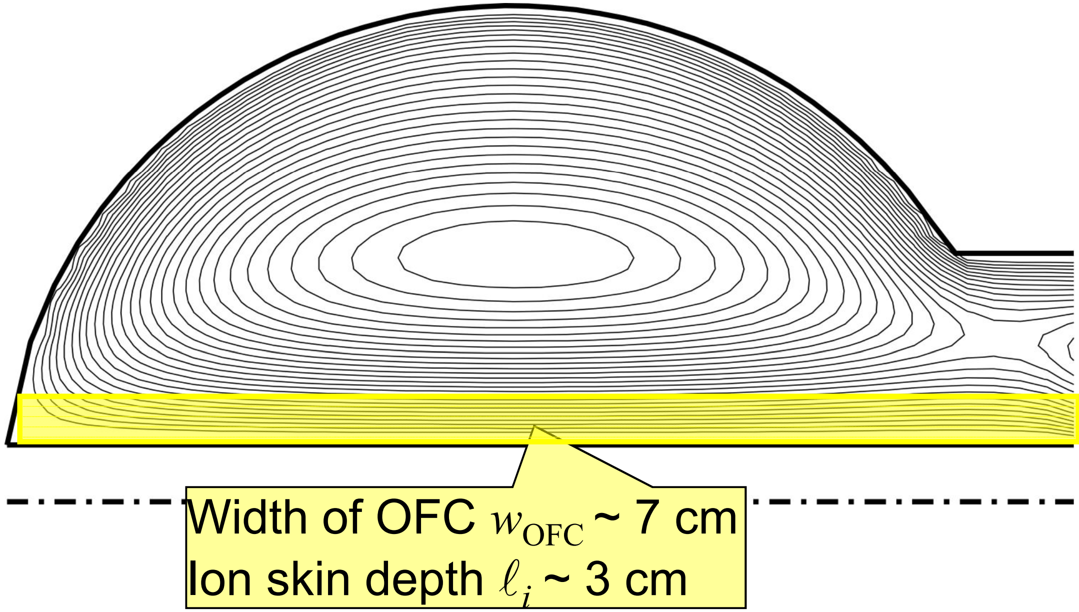

-- Equilibrium has axially elongated, and the flux quantities are principally concentrated on the periphery region due to the hollow current profile.

-- The *q* profile shows a standard tokamak configuration with $q > 6$.

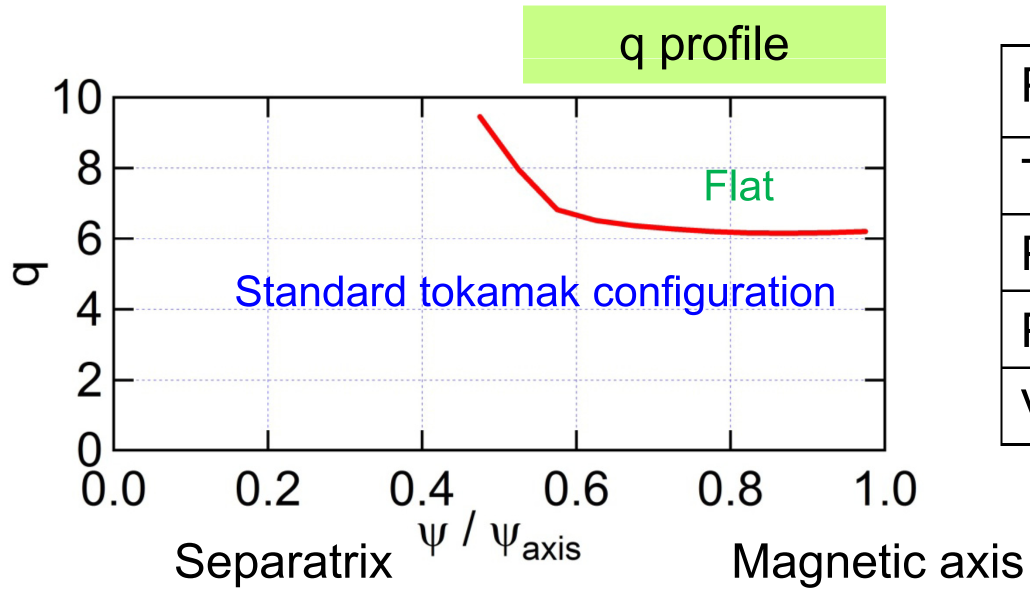

Parameters	Real quantities
Toroidal current I_{tor}	88.1 kA
Poloidal current I_{pol}	15.9 kA
Poloidal flux ψ_{pol}	4.35 mWb
Volume average beta $\langle\beta\rangle$	0.78

Magnetic field and current density profiles at the midplane

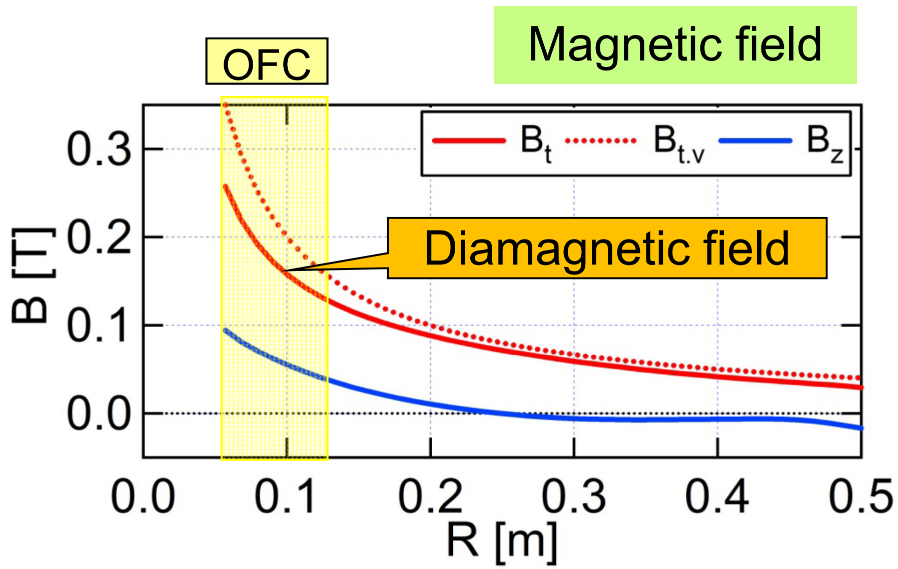

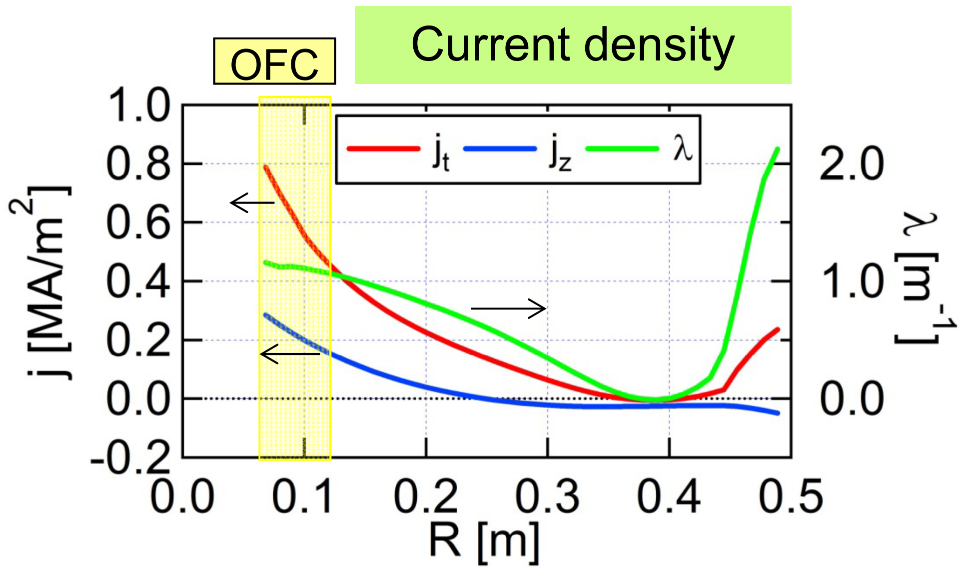

-- Toroidal field B_t has a diamagnetic profile in the whole region.
In particular, the OFC region is significant due to the steep density.

-- Toroidal current density j_t with hollow profile has a maximum value in the OFC region and is slightly negative around R=0.4 m.

-- Parallel current density λ with hollow profile has a maximum value around the outer edge region and is slightly negative around R=0.4 m.

-- The magnetic field and current profiles are consistent with the experiment.

Number density and temperature profiles at the midplane

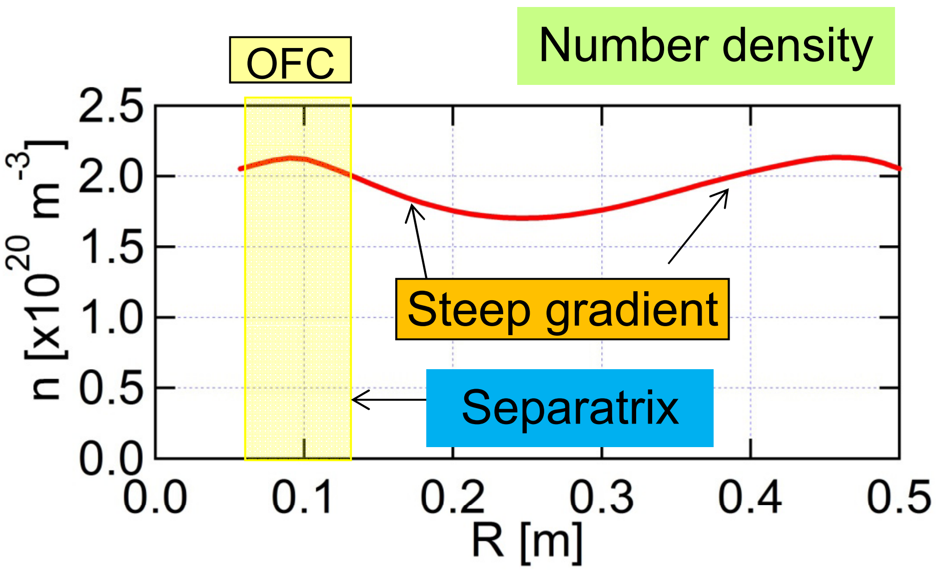

n_{max} = 2.1x10^{20} [m^{-3}], n_{min} = 1.7x10^{20} [m^{-3}]

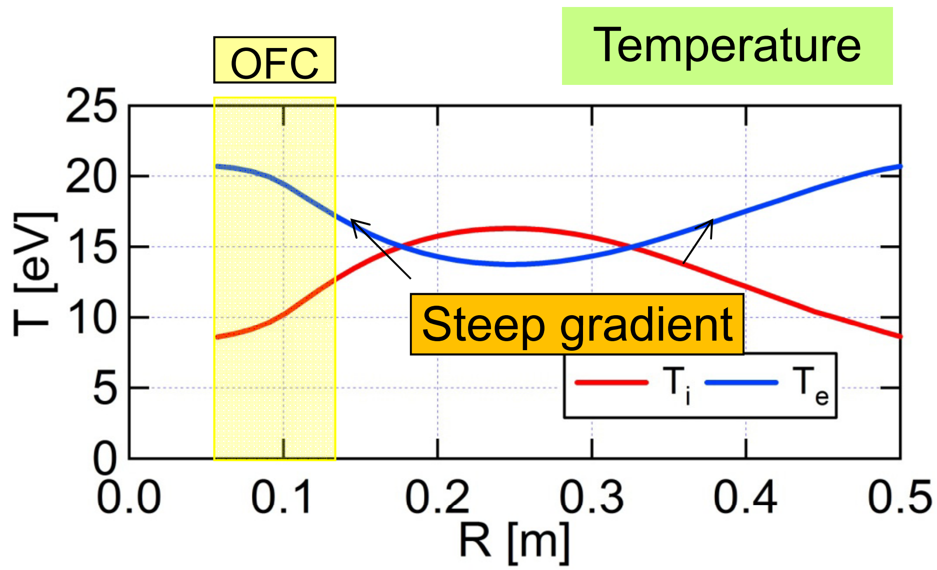

$T_{i.max}$ = 16.3 [eV], $T_{i.min}$ = 8.6 [eV]
$T_{e.max}$ = 20.7 [eV], $T_{e.min}$ = 13.7 [eV]

-- Number density n has a steep gradient scale around the separatrix which is comparable to the ion skin depth.

-- The density gradient in high field side of the experiment is much steeper than that of calculation, and is not so steep in outer edge region.

-- The ion temperature T_i has a peaked profile, and electron temperature T_e has a hollow profile. These profiles are consistent with the experiments.

Flow structures at the midplane

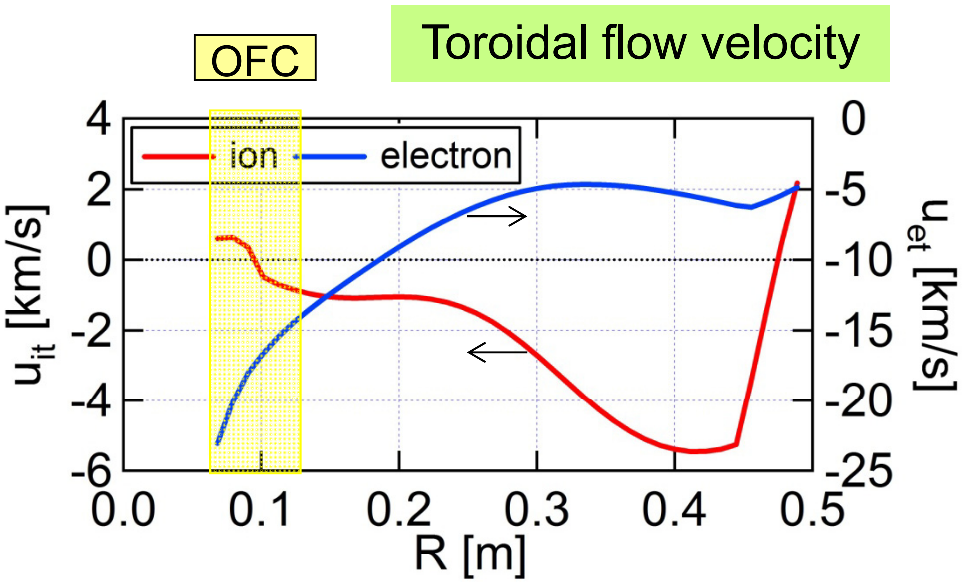

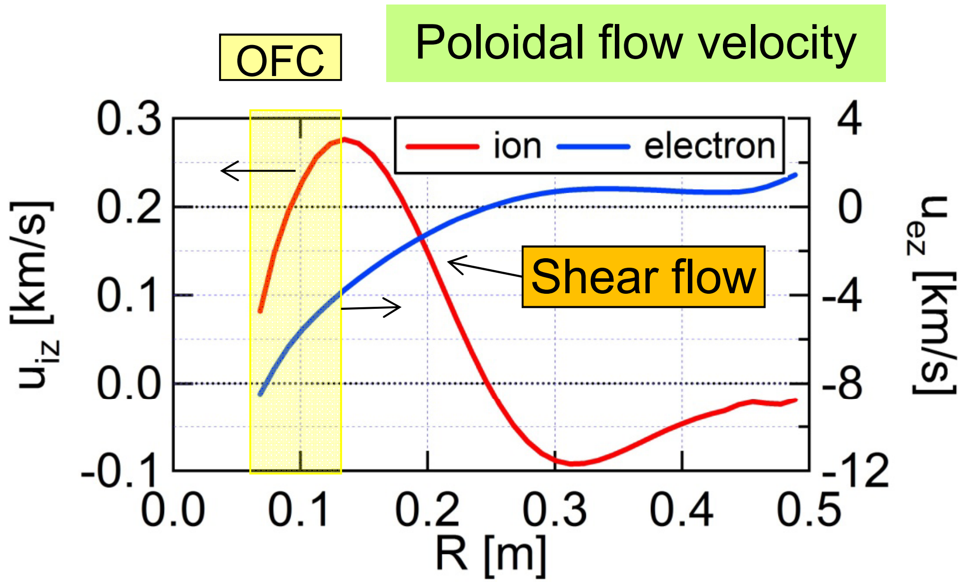

-- The ion flow velocity is the same direction as the electron velocity in the both edge regions, but is the opposite direction to the electron velocity in the core region.

-- The toroidal ion flow velocity is the opposite direction to the toroidal current except in the outer region.

-- Both the toroidal and poloidal currents are carried by both ion and electron flows.

-- The electron fluid mostly moves along the magnetic field.

-- The poloidal Ion flow velocity has a strong shear around the magnetic axis.

Ohm's law and two-fluid effect

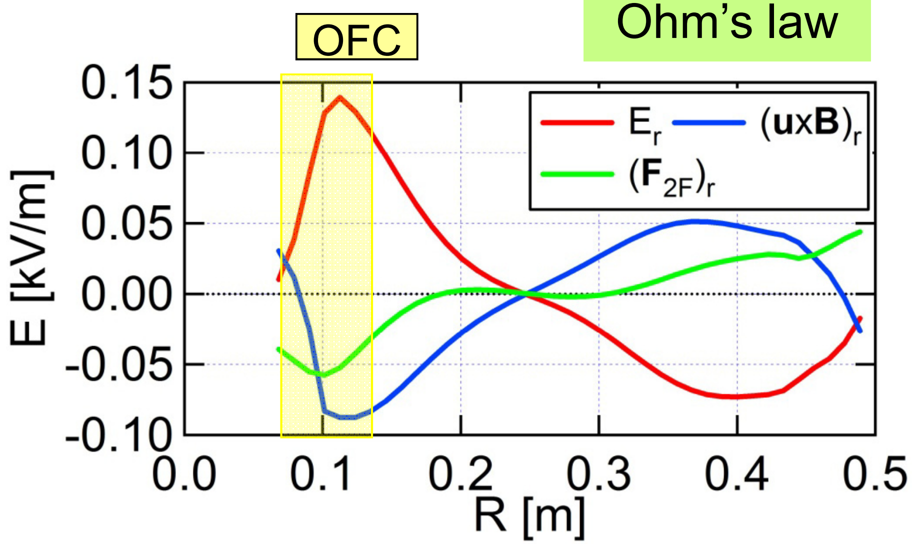

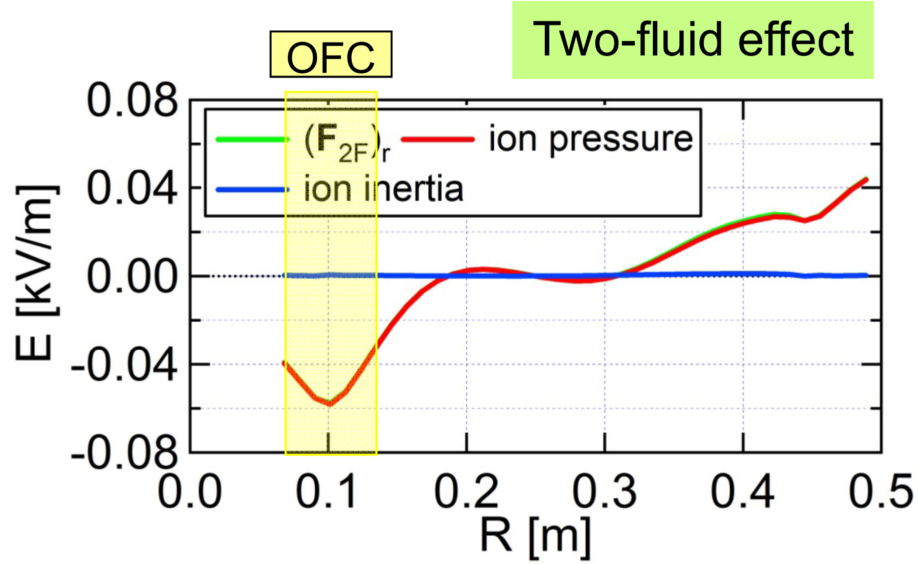

The two-fluid effect is large in a region with the steep density gradient.

The two-fluid effect is due to the ion diamagnetic effect.

Ohm's law: $\boldsymbol{E} + (1/\varepsilon)\boldsymbol{u}_i \times \boldsymbol{B} + \boldsymbol{F}_{2F} = 0$

Two-fluid effect: $\boldsymbol{F}_{2F} = -\nabla p_i / n - \boldsymbol{u}_i \cdot \nabla \boldsymbol{u}_i = \nabla p_e / n - \left(\nabla \times \boldsymbol{B}\right) \times \boldsymbol{B} / n$

Ion diamagnetic effect

Ion inertial effect

Electron pressure

Hall effect

Poloidal component of ion drift velocity

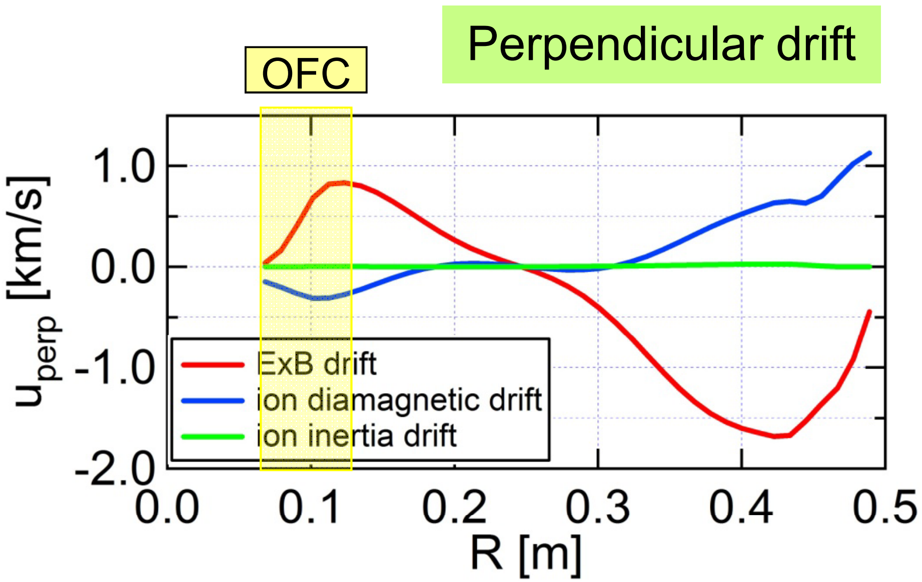

E×**B** drift velocity: $\mathbf{u}_E = \varepsilon \dfrac{\mathbf{E}\times\mathbf{B}}{B^2}$

Diamagnetic drift velocity: $\mathbf{u}_D = \varepsilon \dfrac{\mathbf{B}\times\nabla p_i}{B^2 n}$

Inertial drift velocity: $\mathbf{u}_I = \varepsilon \dfrac{\mathbf{B}\times(\mathbf{u}_i\cdot\nabla\mathbf{u}_i)}{B^2}$

-- The magnitude of ExB drift velocity is comparable to that of ion diamagnetic drift velocity.

-- The ion diamagnetic drift velocity is the opposite direction to the ExB drift velocity which is due to the positive pressure gradient in the OFC region.

Summary

We have obtained the numerical results of the 2-fluid flowing equilibria on the basis of data of the double-pulsing HIST-CHI experiment.

- **The equilibrium has diamagnetic toroidal field, steep density gradient, ion shear flow, and high-β ($<\beta>=78\%$).**

- **The Ion shear flow velocity in the high magnetic field side is the opposite direction to the electron flow velocity due to the ion diamagnetic drift. The currents are carried by both ion and electron flows. The electron fluid mostly moves along the magnetic field.**

- **The two-fluid effect is significant in a region with the steep density gradient due to the ion diamagnetic effect.**

Future work

We will reconstruct more realistic 2-fluid flowing equilibria of HIST in regard to the absolute values of physical quantities and profiles of density and flow velocity.